Quantum coherent dissipation: A glimpse of the "cat"

D. Segale, M. Karavitis, E. Fredj, and V. A. Apkarian[a)]
Department of Chemistry, University of California, Irvine, California 92697

(Received 7 January 2005; accepted 8 February 2005; published online 24 March 2005)

Quantum coherent vibrational relaxation of an impurity strongly coupled to its solid host is demonstrated through four-wave mixing measurements to infer sustained coherence in the bath, which is recognized as a superposition of macroscopically distinct states. © *2005 American Institute of Physics*. [DOI: 10.1063/1.1883634]

Decoherence, to which is ascribed the transition from the quantum dynamics that governs microscopic states to the classicality of the macroscopic world, is a subject of contemporary interest.[1] Its inevitability is manifest in the absence of quantum interference between macroscopically distinct states (QIMDS),[2] more affectionately noted by the absence of Schrödinger's cats in common experience. Yet, "cat"-like states can be expected to prevail at least transiently in the limit of strong coupling, when the communication between a system and its environment is faster than the characteristic periods of motion of the immediate bath, and therefore faster than the pure dephasing or decoherence time. A unique signature for such a realization is the observation of *sustained system coherence despite extensive dissipation*, as we illustrate experimentally for the mechanical process of vibrational relaxation in the solid state. To be clear, prior to presenting the experiments, we give an operational definition of "cat"-states, closely following an exposition due to Leggett.[2]

Schrödinger's measurement paradox rests on two principles;[3] the superposition principle and the linearity of the quantum propagator. The first allows for the preparation of a microsystem in linear combination:

$$|s\rangle = |s_1\rangle + |s_2\rangle \tag{1}$$

which is verifiable through measurement, such as in the two-slit experiment where the screen acts as the position projector $\hat{P}=|x\rangle\langle x|$ to measure intensity at a given point:

$$\mathrm{Tr}[\hat{P}\rho] = s_1^2(x) + s_2^2(x) + 2\,\mathrm{Re}[s_1^*(x)s_2(x)]. \tag{2}$$

The observation of the interference term in (2) leads to the inference of coherence, $\rho_{12}(x)$:

$$\rho_{12}(x) = \langle x|s_1\rangle\langle s_2|x\rangle. \tag{3}$$

Although measurements are carried out over ensembles, in discrete counting measurements, ensuring that the members of the ensemble are well separated in time assures that quantum coherence of the constituent members is measured.

The linearity of the quantum propagator would suggest that if a microsystem were prepared in superposition in the presence of a bath:

$$\chi(t_0) = |s\rangle|B\rangle = (|s_1\rangle + |s_2\rangle)|B\rangle \tag{4}$$

upon interaction, a superposition of the super-system arises:

$$\chi(t) = \chi_1(t) + \chi_2(t) = U(t,t_0)\chi(t_0) = |s_1,B;t\rangle + |s_2,B;t\rangle. \tag{5}$$

Since by definition measurements are local to system coordinates, it is useful to separate out the system coordinate after the interaction, to note that at the time of measurement, t_m, the system and bath are entangled:

$$\chi_1(t_m) + \chi_2(t_m) = |s_1'\rangle|B_1\rangle + |s_2'\rangle|B_2\rangle. \tag{6}$$

The primes identify post-interaction states of the system at $t=t_m$, and recognize that the interaction leads to change of state in the microsystem (transfer of energy, phase, or rotation of coordinates). The interaction also ensures that the distinct $|s_1\rangle$ and $|s_2\rangle$ states will launch their associated baths into distinct histories of evolution: $|B_1\rangle$ and $|B_2\rangle$. By virtue of the entanglement (6), measurements on the system allow inferences about the bath.[4] In particular, the observation of interference in a two-slit measurement now implies coherence in the bath:

$$\rho_{12}(x) = \langle x|s_1'\rangle\langle s_2'|x\rangle\langle B_1|B_2\rangle. \tag{7}$$

The visibility of (system) fringes will decay as the bath–bath correlation decays, a process more commonly identified as pure dephasing. Also, there can be no measurable interference if $|B_1\rangle$ and $|B_2\rangle$ are orthogonal, i.e., if the path taken by the system can be identified with certainty—a result familiarized by Feynman's atomic microscope where $|B_1\rangle$ and $|B_2\rangle$ are states of the "which path?" detector.[5] However, since the two baths have a common origin, $|B;t_0\rangle$, the decay in the bath–bath correlation, or orthogonality, develops continuously in time, on a timescale characteristic of the dynamics of the driven bath. It is during this period that post dissipation coherence may be detected through measurements on the system, with the complementary inference of coherence in the bath.

The superposition (6) is "cat"-like, if $|B_1\rangle$ and $|B_2\rangle$ can be identified as macroscopically distinct states. To qualify as

[a)]Electronic mail: aapkaria@uci.edu

distinct, it is sufficient that they differ by some extensive quantity, such as (but not limited to) energy:

$$\langle E_1\rangle = \langle B_1|H|B_1\rangle \neq \langle B_2|H|B_2\rangle = \langle E_2\rangle. \tag{8}$$

Such an assessment can be made experimentally, in terms of system observables, by measuring dissipation (energy transfer from system to bath):

$$\langle s_1|H|s_1\rangle - \langle s_1'|H|s_1'\rangle \neq \langle s_2|H|s_2\rangle - \langle s_2'|H|s_2'\rangle. \tag{9}$$

The qualification of macroscopic is a matter of degree, the more significant measure being the extent of entanglement, i.e., the number of independent degrees of freedom of a multimode bath that are directly or indirectly entangled with the system. Expanding the instantaneous bath density operator in terms of a suitable orthogonal basis that minimizes off-diagonal contributions (the preferred basis):

$$|B_1\rangle\langle B_2| = \sum_{i=1}^{N} \beta_{i1}\beta_{2i}^{*}|b_i\rangle\langle b_i| + \sum_{i\neq j} \beta_{i1}\beta_{2j}^{*}|b_i\rangle\langle b_j|, \tag{10a}$$

where

$$\beta_{ik} = \langle b_i|B_k\rangle \tag{10b}$$

identifies $(N^2-N)/2$ as the number of independent correlations that must be specified to distinguish the collective coherence from the corresponding classical mixture of states.[6] Although the bath is not directly observed, rudimentary knowledge about its dynamics—such as may be gleaned from classical trajectories—may be sufficient to assess the extent of entanglement. If we insist that cat-dead and cat-alive are strictly orthogonal states, then we should recognize that measurements exhibiting nonvanishing system coherence can only be made during the period of deterministic evolution into orthogonality.[7]

The *coherent superposition of N-nearly orthogonal degrees of freedom belonging to two macroscopically distinct states* is offered as the operative definition of Schrödinger's cat. Such a state will be ephemeral—its observation will be limited either by the duration of time over which the two macroscopic states achieve orthogonality, or by the more common path of decoherence via phase damping. The mechanics of decoherence and the possibilities of its control are the principal motivations for the experiments which we draw upon in the present report.

The experiments are carried out on molecular iodine isolated in the van der Waals solid of Kr, at a doping ratio of 1:4000, at $T=35$ K. We consider the evolution of vibrational coherences on the electronically excited $B(^3\Pi_{0u})$ state of $I_2/Kr(s)$, a system in which the vibrational dynamics has been characterized in great detail through previous pump-probe experiments.[8–10] The equilibrium bond length of I_2 on the B-state is 0.3 Å longer than in the ground $X(^1\Sigma_{0g})$ state. When the excited state is prepared suddenly by optical excitation, the molecular bond stretches by more than 1 Å in its first excursion,[8] and drives the lattice into motion. The rate of energy transfer in this process varies by nearly 3 orders of magnitude depending on the initial excitation energy.[10] Near $\lambda=500$ nm, when the B state is prepared near its gas phase dissociation limit, as many as 40 vibrational quanta are transferred to the lattice in one vibrational period (~300 fs), on a timescale significantly shorter than the period of motion of the fastest lattice phonons (650 fs at the Debye limit in solid Kr).[11] That this strongly dissipative dynamics proceeds by retention of quantum coherence for many periods of motion, we demonstrate through direct measurements.

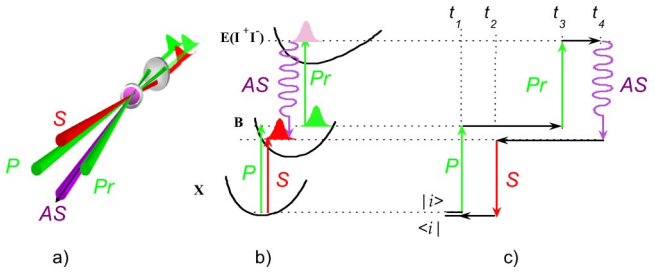

FIG. 1. The measurement: (a) the experimental geometry; (b) along the molecular coordinate, two energetically distinct vibrational packets are launched on the B-state, the P-packet is intercepted by the Pr-pulse, and after a short evolution on the E-state, it is dipole projected on the S-packet; (c) the measured third-order polarization is described by the time-circuit diagram, where coherence signifies periodicity of the system + bath dynamics along the closed circuit.

The measurement paradigm, which relies on electronically resonant time- and frequency-resolved four-wave mixing, has already been introduced.[12] The molecular third-order polarization, $P^{(3)}(t)=\mathrm{Tr}[\mu\rho^{(3)}]$,[13] is measured using three short laser pulses (~30 fs each) propagating along three distinct directions (see Fig. 1). The input pulses are identified as pump (P), probe (Pr) and Stokes (S), which in the present experiment are centered at $\lambda_P=\lambda_{Pr}=540$ nm, $\lambda_S=560$ nm. The bichromophoric coherent anti-Stokes radiation, propagating along $\mathbf{k}_{AS}=\mathbf{k}_P-\mathbf{k}_S+\mathbf{k}_{Pr}$, serves as signal:

$$I_{AS}(t) = [P^{(3)}(k_{AS};t)]^2 = \int dr_{ij} e^{ik_{AS}(r_j-r_i)} P_j^{(3)^*} P_i^{(3)} \tag{11}$$

in which r_i is the coordinate of the ith molecule. The particular component of the molecular polarization selected in this implementation is illustrated in Fig. 1(b) along the molecular (system) coordinate and as a time-circuit diagram on a given molecule [Fig. 1(c)]. The latter diagram transcribes to

$$P_i^{(3)}(t) = \mathrm{Tr}[\hat{\mu}_{BE}\hat{U}(t_4,t_3)\hat{\mu}_{EB}\hat{E}(k_{Pr};t_3)\hat{U}(t_3,t_1)\hat{\mu}_{BX}\hat{E}(k_P;t_1)\rho_{XX}(T)\hat{\mu}_{XB}\hat{E}^*(k_S;t_2)\hat{U}(t_2,t_4)] \tag{12}$$

and can be decomposed into preparation of a vibrational coherence and its projective interrogation.

Starting with the initial thermal density $\rho_{XX}(T)$ consisting of the molecule in its electronic and vibrational ground state in a lattice of thermally occupied phonons, the P- and S-pulses prepare two energetically distinct vibrational wavepackets as a coherence grating:

$$|\varphi_P(\vec{k}_P;t-t_1)\rangle\langle\varphi_S(\vec{k}_S;t-t_2)|$$
$$= \hat{U}(t,t_1)\hat{\mu}_{BX}\hat{E}(k_P;t_1)\rho_{XX}(T)\hat{\mu}_{XB}\hat{E}^*(k_S;t_2)\hat{U}(t_2,t)$$
$$= e^{i(\vec{k}_P-\vec{k}_S)r}|\varphi_P(t-t_1)\rangle\langle\varphi_S(t-t_2)|. \quad (13)$$

Since the electronic resonances are localized on the molecular coordinate (q,p), and the pulsewidths are short in comparison to the characteristic periods of the lattice coordinates $(\mathbf{Q},\mathbf{P})$, the packets are prepared *suddenly* with the lattice in its original configuration:

$$|\varphi_P(t_1)\rangle = \left(\sum_v a_v(t_1)|v\rangle\right)|\mathbf{B};t_0\rangle = |s_1\rangle|\mathbf{B}\rangle, \quad (14a)$$

$$|\varphi_S(t_2)\rangle = \left(\sum_v a_v(t_2)|v\rangle\right)|\mathbf{B};t_0\rangle = |s_2\rangle|\mathbf{B}\rangle, \quad (14b)$$

where the coefficients of the vibrational expansion are given by the usual Franck–Condon factors and resonance condition. The expansion of the system in terms of the vibrational basis of the solvated molecular potential is made as a conceptual convenience, otherwise, the strong dissipation makes the preferred bases the coherent state representation in p,q.[12]

After evolution subject to the global Hamiltonian of system + bath $H_0(q,p;\mathbf{Q},\mathbf{P})$, the coherence grating is read-out with a probe pulse resonant with the $B\leftrightarrow E$ electronic transition. The detection process consists of promoting the P-packet to the E-state as it enters the Franck–Condon window $W(p,q)$ carved out by the Pr-pulse at $t=t_3$, followed by CARS radiation when the S-packet reaches vertical overlap with the packet on the E-state within the anti-Stokes window $W(p'q')$. The resonant scattering process described by the action of the probe pulse, evolution on the E-state, and radiation over the $B\leftrightarrow E$ transition in (12), can be grouped together to define a projector that permits shifts in time and phase space along the system coordinates:[12]

$$\hat{P} \equiv \hat{\mu}_{BE}U(t_4,t_3)\hat{\mu}_{EB}E(k_P;t_3)$$
$$= W(q',p')W(p,q)|q',p';t_4\rangle\langle q,p;t_3|. \quad (15)$$

Accordingly, the observable polarization reduces to the projective measure of the coherence between the *P*- and *S*-packets, with the bath traced out:

$$P^{(3)}(t) = \mathrm{Tr}_B[\hat{P}|\varphi_P(t-t_1)\rangle\langle\varphi_S(t-t_2)|]$$
$$= \mathrm{Tr}[\langle s_2'(t_4)|\hat{P}|s_1'(t_3)\rangle\langle B_2(t_4)|B_1(t_3)\rangle]$$
$$= \langle B_2(t_4)|B_1(t_3)\rangle \int dpdp'dqdq'W(p',q')W(p,q)$$
$$\times\langle s_2'(t_4)|p',q'\rangle\langle p,q|s_1'(t_3)\rangle. \quad (16)$$

Evolution on the E-state during t_{43}, which is limited to the relatively short electronic dephasing time between B- and E-states, plays the important role of overcoming space/time slippage between P- and S-packets.

In Fig. 2, the spectrally dispersed CARS signal is shown as a function of probe delay, t_{31}, with $t_{21}=-40$ fs selected by optimizing the signal. The spectral compositions of the pump and Stokes pulses, along with the anti-Stokes spectral window given by the parametric condition, $\omega=\omega_{Pr}+\omega_{Pr}-\omega_S$, are

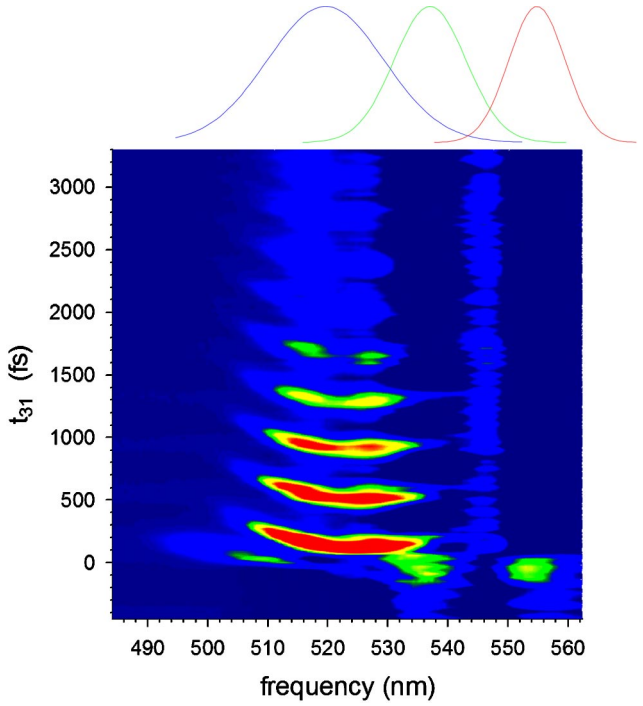

FIG. 2. The spectrally dispersed CARS signal as function of delay between P- and Pr-pulse, t_{31}, with delay between P- and S-pulses fixed at $t_{21}=-40$ fs. The residual scattered laser light along the collected direction has been subtracted. The CARS progression centered at 520 nm is the E-state mediated projection between the two oscillating packets, which splits into the + and − momentum components near the right-turning point of the B-potential (Ref. 14).

indicated above the figure. At these colors, the prepared P- and S-packets are centered on $v=30$ and $v=20$, respectively, (14a) and (14b). Both packets are subject to dissipation: the P-packet loses 300 cm^{-1}/ps, the S-packet loses 100 cm^{-1}/ps.[10] Nevertheless, the coherent signal is observed for ~9 recursions with a periodicity of ~300 fs, which is the vibrational period of iodine on the B-state. A two-dimensional map of the CARS signal at 520 nm is shown in Fig. 3 as a function of delay times t_{21} and t_{31}. The first appearance of the signal is at $t_{31}=180$ fs, indicating that the main contribution to the anti-Stokes signal comes when the probe packet is captured shortly after it passes the right turning point of the B-potential. The maxima in the signal occur when the P-packet is launched 40 fs before the S-packet ($t_{21}=-40$ fs). This delay compensates for the difference in the periods of the packets that arises from the anharmonicity of the molecular potential and nonlinear energy loss upon first collision between molecule and cage.[9,10] The persistence length of the signal along the t_{21} axis establishes the electronic dephasing time between *X* and *B* states of ~100 fs. The measurements contain detailed information regarding energetics and dynamics, which is taken up elsewhere.[13,14] Here, we contend with the gross observation that coherence between the two packets is sustained for ~9 vibrational periods, and note that the decay of the signal as a function of t_{31} follows closely what is observed in single color pump–probe measurements at 540 nm.[8,9] In the latter case, the decay is established to be due to the combination of vibrational amplitude damping (such that the packet falls out of the obser-

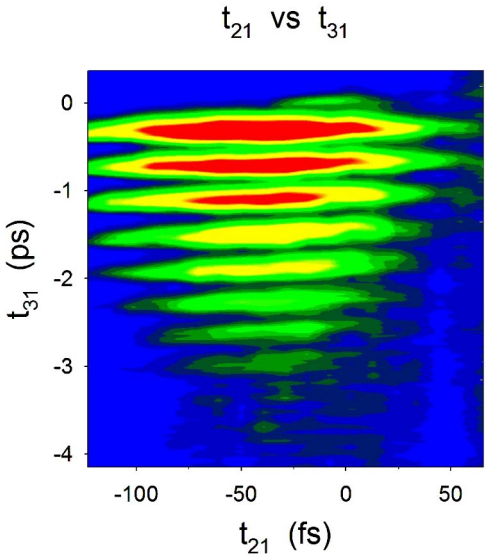

FIG. 3. The 2-D map of the CARS signal ($\lambda_P=\lambda_{Pr}=540$ nm, $\lambda_S=560$ nm, detected at $\lambda_{AS}=520$ nm), as a function of the time delays between P- and S-pulses, t_{21}, and the P- and Pr-pulses, t_{31}.

vation window) and population decay through predissociation.[15] Evidently, the same holds in the present case; rather than being governed by bath–bath overlap, the decay of the signal in time is principally determined by the projective overlap between the two packets in (16). We may conclude that decoherence plays a minor role during the observation, during which $\sim$1000 cm^{-1} of vibrational energy is transferred from the molecule to the lattice. Note, the differential energy loss between the packets is evident from the red shading of the CARS spectra (see Fig. 2), since the parametric condition now dictates that $\omega_{AS}=\omega_{Pr}+(\varepsilon_P-\varepsilon_S)/\hbar$, where ε_P and ε_S are the probed components of the energy distributions in the two packets.

Given the very different rates of energy dissipation, after the first excursion of the molecular bond two distinct baths that differ by $\sim$2kT in their energy content are created. Yet, for the 3 ps duration of the signal, the coherence observed remains limited by the projective overlap of the system wavepackets, and therefore according to (16):

$$\langle B_1(t)|B_2(t)\rangle \approx 1. \tag{17}$$

The bath/bath correlation, which may be decomposed as an overlap in coordinates and a global phase given by the action accumulated over the time-loop in Fig. 1, is maintained.[12,16] We must conclude that the driven modes of the bath that are mechanically coupled to the molecule simultaneously retain coherence.

That a nontrivial coherence must be generated in the bath is established through classical dynamical simulations. Using previously calibrated pair potentials, classical simulations were carried out on a cell of 500 Kr atoms, subject to periodic boundary conditions, with I_2 introduced as a bisubstitutional impurity.[8] At different time intervals, the Cartesian amplitudes were projected on the normal modes of the cell. Typically, after 1 ps of evolution, 12 different normal modes of the bath show occupation numbers n_k of 1 to 2, to conclude that as many orthogonal modes are entangled in the superposition. The subsequent dynamics is well described as that of suddenly displaced, weakly coupled, phonons, as detailed in a prior semiclassical simulation of the closely related system of Cl_2 trapped in solid Ar.[17] In effect, the bath coherence consists of a superposition of $N\geqslant 12$ nearly independent degrees of freedom (10), launched as a phonon packet by the rapid transfer of vibrational energy from the molecule to the lattice. This matches our operative definition of "cat" states.

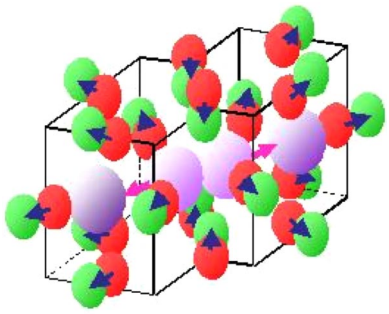

FIG. 4. Illustration of a lattice simultaneously kicked (green) and at rest (red), driven by a molecule simultaneously stretched (green packet in Fig. 1) and compressed (red packet in Fig. 1).

It is useful to state the conclusion in a more physically descriptive picture. The preparation of a molecule in a vibrational superposition is commonplace. The superposition principle (1) allows the preparation of P- and S-packets on the isolated molecule at a delay which corresponds to half of a vibrational period, and therefore allows for a molecule to be simultaneously stretched and compressed [as in Fig. 1(b)]. In the lattice, the strong coupling of the B-state would imply that the host is simultaneously kicked and at rest (5), as illustrated in Fig. 4. The observation of coherence past such a preparation implies a lattice simultaneously driven into two different histories of evolution (6), which is analogous to driving a cat into a state of being simultaneously dead and alive. The cattiness of the prepared superpositions of states, which are distinct by 10 kT in energy, is characterized by the involvement of some 12 independent degrees of freedom. Such processes will likely be ubiquitous in the strong coupling limit, since it takes time for a bath to decohere.

In the experiment selected for this report, dissipation limits the observation. In more extensive studies,[14] it is seen that the onset of decoherence depends sensitively on initial preparations—energy of the packets and their spectral separation—as already reported in a closely related measurement.[12]

[1]W. H. Zurek, Rev. Mod. Phys. **75**, 715 (2003).
[2]A. J. Leggett, J. Phys.: Condens. Matter **14**, R415 (2002).
[3]E. Schrödinger, Naturwiss. **23**, 807 (1935); **23**, 823 (1935); **23**, 844 (1935); for the English translation see, J. D. Trimmer, Proc. Am. Philos. Soc. **124**, 323 (1980).
[4]E. Schrödinger, Probability relations between separated systems, Proc. Cambridge Philos. Soc. **32**, 446 (1936).
[5]S. Durr, T. Nonn, and G. Rempe, Nature (London) **395**, 33, (1998).
[6]Instead of N as defined in (7), Leggett uses a closely related concept of the degree of disconnectivity, D (Ref. 2).
[7]H. Fidder and O. Tapia, Int. J. Quantum Chem. **97**, 670 (2004).
[8]R. Zadoyan, M. Sterling, and V. A. Apkarian, J. Chem. Soc., Faraday Trans. **92**, 1821 (1996).

[9]M. Bargheer, P. Dietrich, K. Donovang, and N. Schwentner, J. Chem. Phys. **111**, 8556 (1999).
[10]M. Bargheer, M. Gühr, P. Dietrich, and N. Schwentner, Phys. Chem. Chem. Phys. **4**, 75 (2002).
[11]J. Almy, J., K. Kizer, R. Zadoyan, and V. A. Apkarian, J. Phys. Chem. A **104**, 3508 (2000).
[12]Z. Bihary, M. Karavitis, and V. A. Apkarian, J. Chem. Phys. **120**, 8144 (2004).
[13]S. Mukamel, *Principles of Nonlinear Optical Spectroscopy* (Oxford University Press, New York, 1999).
[14]D. Segale and V. A. Apkarian, manuscript in preparation.
[15]Pump–probe measurements interrogate the diagonal system density evolving in a single bath.
[16]For a general semiclassical treatment of decoherence in the two-slit experiment, in terms of Gaussian packets, see G. A. Fiete and E. J. Heller, Phys. Rev. A **68**, 022112 (2003).
[17]M. Ovchinnikov and V. A. Apkarian, J. Chem. Phys. **108**, 2277 (1998).